

Superconductivity in transition metal dichalcogenides

Evan Sosenko,^{*} Junhua Zhang,[†] and Vivek Aji[‡]

Department of Physics, University of California, Riverside, California 92521, USA

(Dated: July 22, 2022)

Two dimensional transition metal dichalcogenides entwine interaction, spin-orbit coupling, and topology. Hole-doped systems lack spin degeneracy: states are indexed with spin and valley specificity. This unique structure offers new possibilities for correlated phases and phenomena. We realize an unconventional superconducting pairing phase which is an equal mixture of a spin singlet and the $m = 0$ spin triplet. It is stable against large in-plane magnetic fields, and its topology allows quasiparticle excitations of net nonzero Berry curvature via pair-breaking circularly polarized light.

Introduction: The interplay of spin-orbit interaction and electron-electron interaction is a fertile area of research where new phases of matter and novel phenomena have been theoretically conjectured and experimentally realized [1–7]. Single-layer transition metal group-VI dichalcogenides (TMDs), MX_2 ($\text{M} = \text{Mo}, \text{W}$ and $\text{X} = \text{S}, \text{Se}, \text{Te}$), are direct band gap semiconductors that have all the necessary ingredients to explore this phenomena [8–17]. While sharing the hexagonal crystal structure of graphene, they differ in three important aspects: (1) inversion symmetry is broken, resulting in a gap as opposed to Dirac nodes; (2) spin is coupled to momenta, yielding a large splitting of the valence bands; and (3) the bands near the chemical potential predominantly have the transition metal d -orbital character [18–23].

The nontrivial Berry curvature associated with the bands near the valleys is a consequence of strong spin-orbit coupling enabled by inversion symmetry breaking and heavy elements such as Mo and W. The Berry curvature engenders an effective intrinsic angular momentum associated with the Bloch wave functions. Remarkably, spin-preserving optical transitions between valence and conduction bands are possible, even though the atomic orbitals involved all have a d -character. Furthermore, the valley-dependent sign of the Berry curvature leads to selective photoexcitation: right circular polarization couples to one valley, and left circular polarization to the other. Consequently, this enables a number of valleytronic and spintronic applications that have attracted a lot of attention over the last few years [24–26].

We are primarily interested in exploiting the band structure and valley-contrasting probe afforded by the nontrivial topology in order to study and manipulate correlated phenomena in these systems. In particular, we focus on hole-doped systems, where an experimentally accessible window in energy is characterized by two disconnected pieces of spin non-degenerate Fermi surfaces. One can preferentially excite electrons from either Fermi surface. Since the spins are locked to their valley index, these excitations have specific s_z (where the z -axis is perpendicular to the two-dimensional crystal). We focus on the possible superconducting states and their properties.

Spin-valley locking and its consequence for superconductivity, dubbed Ising superconductivity, has been pre-

viously studied for heavily doped p -type and n -type TMDs [27–31], where Fermi surfaces of each spin are present in each valley. Our focus is the regime of maximal loss of spin degeneracy where the effects are most striking [32]. The two valleys in the energy landscape generically allow two classes of superconducting phases: intervalley pairing with zero center of mass momentum, and intravalley pairing with finite Cooper pair center of mass. Since center-of-symmetry is broken and spin degeneracy is lost, classifications of superconducting states by parity, i.e., singlet vs. triplet, is no longer possible. In this paper, we study both extrinsic and intrinsic superconductivity by projecting the interactions and pairing potential to the topmost valence band. We identify the possible phases, and analyze the nature of the optoelectronic coupling and the response to magnetic fields. Our main conclusions are as follows:

- (1) For both proximity to an s -wave superconductor, and due to local attractive density-density interactions, the leading instability is due to an intervalley paired state, where the Cooper pair is an equal mixture of a spin singlet and the $m = 0$ spin triplet.
- (2) While the valley selectivity of the optical transition is suppressed, it remains finite. Consequently, the two quasiparticles generated by pair-breaking circularly polarized light are correlated such that one is in the valence band of one valley and the conduction band of the other. The valley and bands are determined by the polarity of incident light.
- (3) The quasiparticles generated in (2) both have the same charge and Berry curvature. Thus an anomalous Hall effect is anticipated as the two travel in the same direction transverse to an applied electric field.
- (4) An in-plane magnetic field tilts the spin, modifying the internal structure of the Cooper pair, however, no pair-breaking is induced in the absence of scalar impurities. The suppression of the effective interaction leads to a parametric reduction of the transition temperature. In the presence of scalar impurities, pair-breaking is enabled, but the associated critical magnetic field is large.

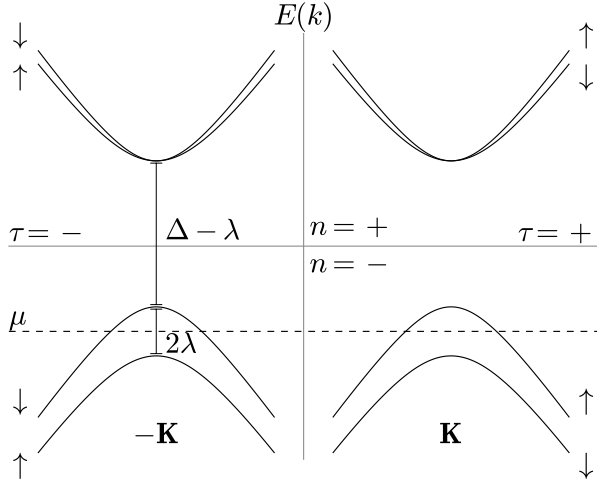


Figure 1. Energy bands for WSe_2 as given by equation (2) with $at = 3.939 \text{ eV \AA}^{-1}$, $\Delta = 1.60 \text{ eV}$, and $\lambda = 0.23 \text{ eV}$. Each valley is centered at $\pm \mathbf{K}$ relative to the center of the Brillouin zone. The energy for a given band depends only on the distance k measured from the valley center.

Model: The TMD system is described by the effective tight-binding, low-energy, two-valley Hamiltonian [25],

$$H_\tau^0(\mathbf{k}) = at(\tau k_x \sigma_x + k_y \sigma_y) \otimes I_2 + \frac{\Delta}{2} \sigma_z \otimes I_2 - \lambda \tau (\sigma_z - 1) \otimes S_z. \quad (1)$$

The operators σ_i are Pauli operators acting on the two Bloch orbital states $|v_{\tau s}^\nu(\mathbf{k})\rangle$ (indexed by $\nu = \pm$ labeling $|d_{x^2-y^2}\rangle + i\tau|d_{xy}\rangle$ and $|d_{z^2}\rangle$) such that $\sigma_z|v_{\tau s}^\pm(\mathbf{k})\rangle = \pm|v_{\tau s}^\pm(\mathbf{k})\rangle$. The valley index $\tau = \pm$, corresponding to the $\pm \mathbf{K}$ points, and the spin index $s = \pm$ (or $s = \uparrow\downarrow$), corresponding to the z -component of the spin through $s_z = s/2$, are good quantum numbers. The momentum \mathbf{k} is measured from the valley center, i.e., for a given valley, the total momentum relative to the center of the Brillouin zone is $\mathbf{k} + \tau \mathbf{K}$. The energy gap is Δ , the spin splitting in the valence band is 2λ , the lattice constant is a , and t is the effective hopping integral.

The energy spectrum,

$$E_{\tau s}^n(k) = \frac{1}{2} \left(\lambda \tau s + n \sqrt{(2atk)^2 + (\Delta - \lambda \tau s)^2} \right), \quad (2)$$

with $k = |\mathbf{k}|$ and $n = 1$ ($n = -1$) indexing the conduction (valence) band is shown in figure 1.

We focus on doped systems such that the chemical potential μ lies in the upper valence bands. Within each band, the Bloch basis eigenstates are written in terms of the orbital states as elements on the Bloch sphere,

$$|u_{\tau s}^n(k, \phi)\rangle = \cos \frac{\theta_{\tau s}^n(k)}{2} |v_{\tau s}^+(k, \phi)\rangle + e^{-i\tau\phi} \sin \frac{\theta_{\tau s}^n(k)}{2} |v_{\tau s}^-(k, \phi)\rangle, \quad (3)$$

where $k_x + i\tau k_y = k e^{i\tau\phi}$ and

$$\tan \frac{\theta_{\tau s}^n(k)}{2} = \frac{atk}{\frac{\Delta}{2} - E_{\tau s}^{-n}(k)} = \frac{atk}{E_{\tau s}^n(k) - E_{\tau s}^-(0)}. \quad (4)$$

The polar angle on the Bloch sphere of the conduction and valence bands are related by $\theta_{\tau s}^-(k) - \theta_{\tau s}^+(k) = \tau\pi$. The mapping of the energy band to the Bloch sphere, parametrized by (θ, ϕ) , encodes the topological character: as one moves from the node out to infinity, the states sweep either the northern or southern hemisphere with a chirality determined by the Berry curvature.

Superconductivity: We consider two approaches to realizing a superconducting state. First, we assume a proximity induced state obtained by layering a TMD on an s -wave superconductor. Second, we study an intrinsic correlated phase arising from density-density interactions.

We use $d_{\tau s}^\nu(\mathbf{k})$ as the annihilation operator for tight-binding d -orbital states, and $c_{\tau s}^n(\mathbf{k})$ for the eigenstates of the non-interacting Hamiltonian, $\lambda_{\mathbf{k}}$ for the energy dispersion for Bogoliubov quasiparticles, and $\Delta_{\mathbf{k}}$ for the superconducting gap function.

Induced State: A proximity s -wave superconductor will inject Cooper pairs according to

$$H^V = \sum_{\mathbf{k}, \nu, \tau} B_\nu^* d_{-\tau\downarrow}^\nu(-\mathbf{k}) d_{\tau\uparrow}^\nu(\mathbf{k}) + \frac{\varepsilon}{2} + \text{h.c.} \quad (5)$$

The coupling constants B_ν and the overall constant ε depend on the material interface [33]. Using the abbreviated notation $c_{\mathbf{k}\alpha} = c_{\tau s}^n(\mathbf{k})$, with $\alpha = \uparrow\downarrow$ for $\tau = s = \pm$, projecting onto the upper valence bands yields,

$$P_{\tau s}^{n--}(H^0 + H^V - \mu N) = \sum_{\mathbf{k}, \alpha} \xi_{\mathbf{k}} c_{\mathbf{k}\alpha}^\dagger c_{\mathbf{k}\alpha} - \sum_{\mathbf{k}} \left(\Delta_{\mathbf{k}}^* c_{-\mathbf{k}\downarrow} c_{\mathbf{k}\uparrow} + \Delta_{\mathbf{k}} c_{\mathbf{k}\uparrow}^\dagger c_{-\mathbf{k}\downarrow}^\dagger \right) + \varepsilon, \quad (6)$$

where $\xi_{\mathbf{k}} = E_{\tau\uparrow}^-(|\mathbf{k}|) - \mu$ and the effective BCS gap function is

$$\Delta_{\mathbf{k}} = \frac{1}{2} (B_+ + B_-) + \frac{1}{2} (B_+ - B_-) \cos \theta_{\mathbf{k}}, \quad (7)$$

with $\theta_{\mathbf{k}} = \theta_{\tau\uparrow}^-(|\mathbf{k}|)$. This form is identical to the standard BCS Hamiltonian with an effective spin index α . However, the spin state of the Cooper pair is an equal superposition of the singlet and the $m = 0$ component of spin triplet. The corresponding quasiparticle eigenstates are $\gamma_{\mathbf{k}\alpha} = \alpha \cos \beta_{\mathbf{k}} c_{\mathbf{k}\alpha} + \sin \beta_{\mathbf{k}} c_{-\mathbf{k}, -\alpha}^\dagger$, with energies $\lambda_{\mathbf{k}} = \pm \sqrt{\xi_{\mathbf{k}}^2 + \Delta_{\mathbf{k}}^2}$, where $\cos 2\beta_{\mathbf{k}} = \xi_{\mathbf{k}}/\lambda_{\mathbf{k}}$. Note that if $B_+ = B_-$, then $\Delta_{\mathbf{k}}$ is a constant and independent of \mathbf{k} . Even when B_+ and B_- are different, the constant term dominates. Before exploring the nature of this state, we analyze the case of intrinsic superconductivity, and show that the same state is energetically preferred.

Intrinsic Phase: For a local attractive density-density interaction (e.g. one mediated by phonons), the potential is $V \simeq \frac{1}{2} \sum_{\mathbf{R}, \mathbf{R}'} v_{\mathbf{R}\mathbf{R}'} n_{\mathbf{R}} n_{\mathbf{R}'}$, with $v_{\mathbf{R}\mathbf{R}'} = v_0 \delta_{\mathbf{R}\mathbf{R}'}$ and $n_{\mathbf{R}}$ the total Wannier electron density at lattice vector \mathbf{R} . Projecting onto states near the chemical potential gives

$$P_{\tau=s}^{n=-} (H^V) = \sum_{\mathbf{k}, \mathbf{k}'} v(\mathbf{k}' - \mathbf{k}) \times \left(A_{\mathbf{k}\mathbf{k}'}^2 c_{\mathbf{k}'\uparrow}^\dagger c_{-\mathbf{k}'\uparrow}^\dagger c_{-\mathbf{k}\uparrow} c_{\mathbf{k}\uparrow} + A_{\mathbf{k}'\mathbf{k}}^2 c_{\mathbf{k}'\downarrow}^\dagger c_{-\mathbf{k}'\downarrow}^\dagger c_{-\mathbf{k}\downarrow} c_{\mathbf{k}\downarrow} + 2|A_{\mathbf{k}\mathbf{k}'}|^2 c_{\mathbf{k}'\uparrow}^\dagger c_{-\mathbf{k}'\downarrow}^\dagger c_{-\mathbf{k}\downarrow} c_{\mathbf{k}\uparrow} \right), \quad (8)$$

where

$$A_{\mathbf{k}\mathbf{k}'} = e^{i(\phi_{\mathbf{k}'} - \phi_{\mathbf{k}})} \sin \frac{\theta_{\mathbf{k}'}}{2} \sin \frac{\theta_{\mathbf{k}}}{2} + \cos \frac{\theta_{\mathbf{k}'}}{2} \cos \frac{\theta_{\mathbf{k}}}{2}. \quad (9)$$

The first two terms in equation (8) lead to intravalley pairing, and the third to intervalley pairing. We analyze the possible states within mean field theory. The BCS order parameter is

$$\chi = v_0 \sum_{\mathbf{k}} g_{\mathbf{k}}^* \langle c_{-\mathbf{k}\alpha} c_{\mathbf{k}\alpha} \rangle, \quad (10)$$

where the form of $g_{\mathbf{k}}$ depends on the particular pairing channel. The resulting Hamiltonian has the same form as the BCS Hamiltonian in equation (6) but with an effective $\Delta_{\mathbf{k}} = g_{\mathbf{k}} \chi$. The intravalley pairing has three symmetry channels, with the couplings given by $2g_{\mathbf{k}} = 1 + \cos \theta_{\mathbf{k}}$, $\sqrt{2}e^{-i\phi_{\mathbf{k}}} g_{\mathbf{k}} = \sin \theta_{\mathbf{k}}$ and $2e^{-2i\phi_{\mathbf{k}}} g_{\mathbf{k}} = 1 - \cos \theta_{\mathbf{k}}$. For these channels, since $\langle c_{-\mathbf{k}\alpha} c_{\mathbf{k}\alpha} \rangle = -\langle c_{\mathbf{k}\alpha} c_{-\mathbf{k}\alpha} \rangle$, relabeling $\mathbf{k} \rightarrow -\mathbf{k}$ in the sum gives $\chi = 0$ [34]. The intervalley pairing also has three symmetry channels: $g_{\mathbf{k}} = \sqrt{2}$, $g_{\mathbf{k}} = \sqrt{2} \cos \theta_{\mathbf{k}}$, and $g_{\mathbf{k}} = \sqrt{2} \sin \theta_{\mathbf{k}} \hat{\mathbf{k}}$. Of the three, the constant valued channel is dominant [35]. This is to be expected, as the local density-density interaction leads to the largest pairing for electrons of opposite spins. Since the intravalley processes have the same spin, they are disfavored as compared to the intervalley pairing.

The key features of the intrinsic superconducting state are identical to the proximally induced case when density-density interactions dominate. We restrict further analysis to that case, and turn to the question of pair-breaking phenomena induced either by optical or magnetic fields.

Optoelectronic coupling: The non-interacting system displays valley selective optical excitations. Light of a particular polarization only couples to one valley. Since the superconducting state is a coherent condensate admixing the two valleys, we address whether pair-breaking displays similar valley selectivity. In particular, we explore whether or not the two quasiparticles generated by circularly polarized light, with total energy larger than $\Delta + \Delta_{\mathbf{k}}$, occupy opposite valleys, with one in the conduction band and the other in the valence band.

The optical excitations arise from the Berry curvature, which acts as an effective angular momentum. The electromagnetic potential \mathbf{A} , with polarization vector $\boldsymbol{\epsilon}$, is introduced using minimal coupling,

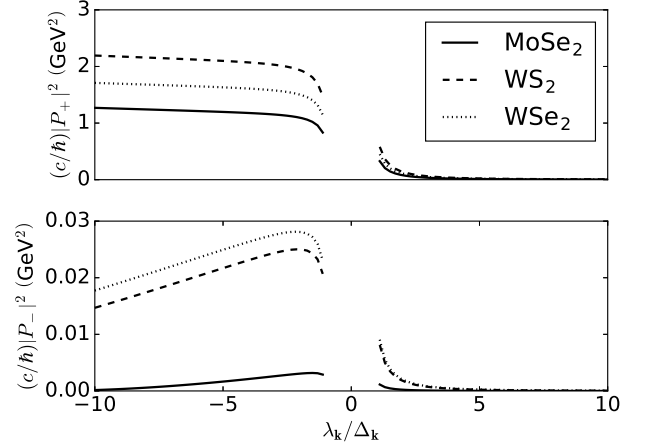


Figure 2. Optical transition rate matrix elements $|P_{\pm}|^2$ in the superconducting phase as a function of the ratio of the quasiparticle energy $\lambda_{\mathbf{k}}$ to the superconducting gap $\Delta_{\mathbf{k}}$. Material parameters for MoSe₂, WS₂, and WSe₂ are given in [25] and a gap of $\Delta_{\mathbf{k}} = 7.5$ meV is chosen for illustrative purposes. The order-of-magnitude contrast between $|P_{+}|^2$ and $|P_{-}|^2$ causes the optical-valley selectivity.

$H_{\tau s}^{\nu\nu'}(\mathbf{k}) \rightarrow H_{\tau s}^{\nu\nu'}(\mathbf{k} + e\mathbf{A})$, where, in the dipole approximation, $\mathbf{A} = 2 \text{Re} \epsilon A_0 e^{-i\omega t}$. This yields a perturbed Hamiltonian $H \rightarrow H + H^A$, where $H^A = H' e^{-i\omega t} + H'^{\dagger} e^{i\omega t}$, with

$$H' = \sum_{\mathbf{k}, \tau, s} H'_{\tau} d_{\tau s}^{-\dagger}(\mathbf{k}) d_{\tau s}^{+}(\mathbf{k}) - \sum_{\mathbf{k}, \tau, s} H'_{-\tau} d_{\tau s}^{+\dagger}(\mathbf{k}) d_{\tau s}^{-}(\mathbf{k}), \quad (11)$$

and $H'_{\tau} = ateA_0 (\tau \hat{\mathbf{x}} + i \hat{\mathbf{y}}) \cdot \boldsymbol{\epsilon}$. The transition rate is proportional to the modulus-squared of the optical matrix elements, $\mathbf{P}_{\tau s}^{nn'}(\mathbf{k})$, defined by

$$H^A = \sum_{\mathbf{k}, \tau, s} \frac{eA_0}{m_0} \boldsymbol{\epsilon} \cdot \mathbf{P}_{\tau s}^{nn'}(\mathbf{k}) c_{\tau s}^{n\dagger}(\mathbf{k}) c_{\tau s}^{n'}(\mathbf{k}). \quad (12)$$

For circularly polarized light, in the absence of superconductivity, $\boldsymbol{\epsilon}_{\pm} = (\hat{\mathbf{x}} \pm i \hat{\mathbf{y}}) / \sqrt{2}$ and

$$\boldsymbol{\epsilon}_{\pm} \cdot \mathbf{P}_{\tau s}^{+-}(\mathbf{k}) = \mp \tau \sqrt{2} a t m_0 e^{\pm i\phi} \sin^2 \frac{\theta_{\tau s}^{\mp}(k)}{2}. \quad (13)$$

The transition rate matrix elements for optical excitations from the BCS ground state are given by equation (13) multiplied by a coherence factor $\sin \beta_{\mathbf{k}}$. Since $\theta_{\tau s}^{-}(k) - \theta_{\tau s}^{+}(k) = \tau\pi$, switching either the valley or polarization transforms $\sin \rightarrow \cos$ in equation (13), giving matrix elements $|P_{\pm}| = |\boldsymbol{\epsilon}_{\pm} \cdot \mathbf{P}_{\tau s}^{+-}(\mathbf{k}) \sin \beta_{\mathbf{k}}|$ corresponding to matching (P_{+}) or mismatching (P_{-}) polarization-valley indexes. For a given valley, a chosen polarization of light couples more strongly than the other, as is evident comparing $|P_{+}|^2$ to $|P_{-}|^2$ and shown in figure 2. For incident light with energy $\Delta + |\lambda_{\mathbf{k}}|$, right circularly

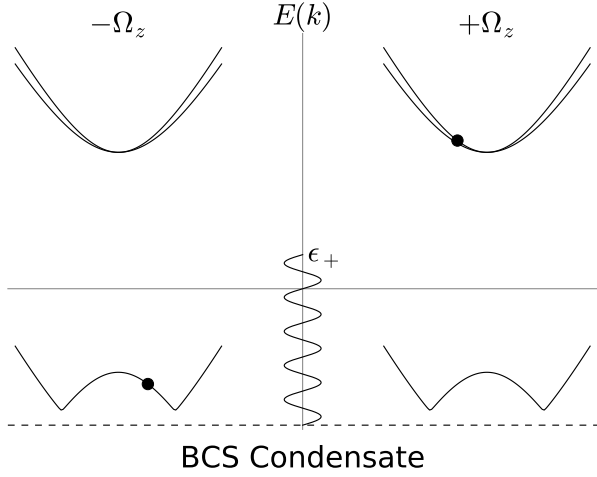


Figure 3. Pair-breaking by right circularly polarized light leads to an electron in the conduction band of the right valley and a partner in the valence band of the left valley. The valleys interchange for left circularly polarized light.

polarized light (+) has a higher probability of promoting a quasiparticle to the right conduction band, as reflected in the larger matrix element $|P_+|^2 \gg |P_-|^2$. As depicted in figure 3, the partner of the Cooper pair is in the valence band in the opposite valley. The other valley has the opposite dependence on polarization.

This key new result opens the door for valley control of excitations from a coherent ground state. For example, the two quasiparticles have the same charge and Berry curvature (see below). In the presence of an electric field, they both acquire the same transverse anomalous velocity. Thus, in contrast to the response in the normal state, an anomalous Hall effect is anticipated with no accompanying spin current.

Berry curvature: The Berry curvature in the non-interacting crystal for left and right circularly polarized (ϵ_{\pm}) optical excitations for a given \mathbf{k} is $\pm 2\Omega_{\pm}^{\uparrow}(k)$, where

$$\Omega_{\tau s}^n(k) = \hat{\mathbf{z}} \cdot \Omega_{\tau s}^n(\mathbf{k}), \quad (14a)$$

$$= -n\tau \left[\frac{1}{2k} \frac{\partial}{\partial k} \theta_{\tau s}^n(k) \right] \sin \theta_{\tau s}^n(k), \quad (14b)$$

$$= -n\tau \frac{2(at)^2 (\Delta - \lambda\tau s)}{\left[(2atk)^2 + (\Delta - \lambda\tau s)^2 \right]^{3/2}}. \quad (14c)$$

The BCS ground state [36] is

$$|\Omega\rangle = \prod_{\mathbf{k}} \text{csc } \beta_{\mathbf{k}} \gamma_{\mathbf{k}\uparrow} \gamma_{-\mathbf{k}\downarrow} |0\rangle, \quad (15a)$$

$$= \prod_{\mathbf{k}} \left(\cos \beta_{\mathbf{k}} - \sin \beta_{\mathbf{k}} c_{\mathbf{k}\uparrow}^{\dagger} c_{-\mathbf{k}\downarrow}^{\dagger} \right) |0\rangle. \quad (15b)$$

This superconducting state is built up from the quasiparticle eigenstates, $|\mathbf{k}\rangle = \text{csc } \beta_{\mathbf{k}} \gamma_{\mathbf{k}\uparrow} \gamma_{-\mathbf{k}\downarrow} |0\rangle$, of the \mathbf{k} -dependent Hamiltonian $\lambda_{\mathbf{k}} \left(\gamma_{\mathbf{k}\uparrow}^{\dagger} \gamma_{\mathbf{k}\uparrow} + \gamma_{-\mathbf{k}\downarrow}^{\dagger} \gamma_{-\mathbf{k}\downarrow} \right)$. The z -

component of the Berry curvature of the correlated state is zero,

$$\hat{\mathbf{z}} \cdot i \nabla_{\mathbf{k}} \times \langle \mathbf{k} | \nabla_{\mathbf{k}} | \mathbf{k} \rangle = \Omega_{+\uparrow}^-(k) + \Omega_{-\downarrow}^+(-k) = 0. \quad (16)$$

A single optically excited state in the left valley for a given \mathbf{k} is $c_{+\uparrow}^{\dagger}(\mathbf{k}) c_{+\uparrow} | \mathbf{k} \rangle$, which has a Berry curvature $+2 \sin^6 \beta_{\mathbf{k}} \Omega_{+\uparrow}^+(k)$. The corresponding excitation in the right valley has a Berry curvature of the same magnitude but opposite sign.

Effect of in-plane magnetic field: We briefly discuss the pair-breaking effects of an in-plane magnetic field and non-magnetic disorder. (The details are presented elsewhere [37].) The superconducting state exhibits an anomalous magnetic response due to the large spin-orbit interaction and spin splitting 2λ . Unlike conventional superconductors, where a uniform magnetic field leads to pair-breaking from spin paramagnetism, here the Zeeman coupling from an in-plane magnetic field in the clean system modifies the spin structure of the Cooper pair and parametrically suppresses T_c . Modification of the effective coupling, rather than pair-breaking, causes this phenomena. While, in compliance with Anderson's theorem, the lack of pair-breaking for non-magnetic impurities is recovered at zero field (since time reversal symmetry is preserved), the transition is indeed suppressed by a pair-breaking effect from the combination of the magnetic field and scalar impurities.

The pair-breaking effect is characterized by the parameter $\delta_c = \tau_0^{-1} \left(\mu_B H_c^{\parallel} / \lambda \right)^2$, where μ_B is the Bohr magneton and τ_0^{-1} is the collision rate resulting from the scalar disorder potential. Note that for a clean system, where $\tau_0 \rightarrow \infty$, we recover the result that there is no pair-breaking. Assuming a continuous phase transition induced by the magnetic field, the pair-breaking equation at temperature T is $\log(T_c'/T) = \psi(1/2 + \delta_c/2\pi k_B T) - \psi(1/2)$, where $\psi(z)$ is the digamma function, T_c' is the transition temperature in the clean system (weakly suppressed by the in-plane field), and k_B is the Boltzmann constant. This equation determines the upper critical field $H_c^{\parallel}(T)$ as a function of temperature. Clearly, the upper critical field is greatly enhanced by the large spin-orbit interaction. At zero temperature, the upper critical field is approximately $\mu_B H_c^{\parallel}(0) = \lambda \sqrt{2\pi k_B T_c' \tau_0} e^{\psi(1/2)}$.

Conclusions: In this letter, we report on the nature of the superconducting state of hole-doped TMDs. Remarkably, the correlated state inherits the valley contrasting phenomena of the non-interacting state. While the magnitude is smaller, pair-breaking produces quasiparticles that have the same Berry curvature, and hence the same anomalous velocity. Thus one predicts an anomalous Hall response unlike the valley Hall response observed in MoSe_2 .

Spin-valley locking leads to large critical magnetic fields. A similar phenomena was recently reported in

heavily hole-doped (beyond the spin-split gap) NbSe₂ [28]. In the new regime, where only one band per valley intersects the chemical potential, no pair-breaking occurs for in-plane fields unless disorder is present.

While systematic synthesis and characterization of hole-doped systems is still in its early stages, the fact that other two-dimensional compounds and their bulk counterparts are known to be superconducting [38] provides impetus to explore this novel phenomena.

Acknowledgments: The software developed [39] and used [40] for this work and the included figures is available freely online. We thank Michael Phillips for useful discussions. We acknowledge the support of the Army Research Office through the grant ARO W911NF1510079.

* evan.sosenko@email.ucr.edu; <https://evansosenko.com>

† junhua.zhang@ucr.edu

‡ vivek.aji@ucr.edu

- [1] F. D. M. Haldane, *Phys. Rev. Lett.* **61**, 2015 (1988).
- [2] C. L. Kane and E. J. Mele, *Phys. Rev. Lett.* **95**, 226801 (2005).
- [3] B. A. Bernevig and S.-C. Zhang, *Phys. Rev. Lett.* **96**, 106802 (2006).
- [4] M. König, S. Wiedmann, C. Brüne, A. Roth, H. Buhmann, L. W. Molenkamp, X.-L. Qi, and S.-C. Zhang, *Science* **318**, 766 (2007).
- [5] M. Z. Hasan and C. L. Kane, *Rev. Mod. Phys.* **82**, 3045 (2010).
- [6] X.-L. Qi and S.-C. Zhang, *Rev. Mod. Phys.* **83**, 1057 (2011).
- [7] W. Witczak-Krempa, G. Chen, Y. B. Kim, and L. Balents, *Annual Review of Condensed Matter Physics* **5**, 57 (2014), <https://dx.doi.org/10.1146/annurev-conmatphys-020911-125138>.
- [8] B. Radisavljevic, A. Radenovic, J. Brivio, V. Giacometti, and A. Kis, *Nat Nano* **6**, 147 (2011).
- [9] Z. Y. Zhu, Y. C. Cheng, and U. Schwingenschlögl, *Phys. Rev. B* **84**, 153402 (2011).
- [10] Y. Zhang, J. Ye, Y. Matsushashi, and Y. Iwasa, *Nano Letters* **12**, 1136 (2012), pMID: 22276648, <https://dx.doi.org/10.1021/nl2021575>.
- [11] Q. H. Wang, K. Kalantar-Zadeh, A. Kis, J. N. Coleman, and M. S. Strano, *Nat Nano* **7**, 699 (2012).
- [12] J. T. Ye, Y. J. Zhang, R. Akashi, M. S. Bahramy, R. Arita, and Y. Iwasa, *Science* **338**, 1193 (2012).
- [13] W. Bao, X. Cai, D. Kim, K. Sridhara, and M. S. Fuhrer, *Applied Physics Letters* **102**, 042104 (2013), <https://dx.doi.org/10.1063/1.4789365>.
- [14] F. Zahid, L. Liu, Y. Zhu, J. Wang, and H. Guo, *AIP Advances* **3**, 052111 (2013), <https://dx.doi.org/10.1063/1.4804936>.
- [15] E. Cappelluti, R. Roldán, J. A. Silva-Guillén, P. Ordejón, and F. Guinea, *Phys. Rev. B* **88**, 075409 (2013).
- [16] X. Xu, W. Yao, D. Xiao, and T. F. Heinz, *Nat Phys* **10**, 343 (2014), review.
- [17] J. Lee, K. F. Mak, and J. Shan, (2015), [arXiv:1508.03068 \[cond-mat.mes-hall\]](https://arxiv.org/abs/1508.03068).
- [18] R. A. Bromley, R. B. Murray, and A. D. Yoffe, *Journal of Physics C: Solid State Physics* **5**, 759 (1972).
- [19] T. Böker, R. Severin, A. Müller, C. Janowitz, R. Manzyke, D. Voß, P. Krüger, A. Mazur, and J. Pollmann, *Phys. Rev. B* **64**, 235305 (2001).
- [20] K. F. Mak, C. Lee, J. Hone, J. Shan, and T. F. Heinz, *Phys. Rev. Lett.* **105**, 136805 (2010).
- [21] A. Splendiani, L. Sun, Y. Zhang, T. Li, J. Kim, C.-Y. Chim, G. Galli, and F. Wang, *Nano Letters* **10**, 1271 (2010), pMID: 20229981, <https://dx.doi.org/10.1021/nl903868w>.
- [22] A. Kormányos, V. Zólyomi, N. D. Drummond, P. Rakyta, G. Burkard, and V. I. Fal'ko, *Phys. Rev. B* **88**, 045416 (2013).
- [23] G.-B. Liu, W.-Y. Shan, Y. Yao, W. Yao, and D. Xiao, *Phys. Rev. B* **88**, 085433 (2013).
- [24] D. Xiao, M.-C. Chang, and Q. Niu, *Rev. Mod. Phys.* **82**, 1959 (2010).
- [25] D. Xiao, G.-B. Liu, W. Feng, X. Xu, and W. Yao, *Phys. Rev. Lett.* **108**, 196802 (2012).
- [26] K. F. Mak, K. L. McGill, J. Park, and P. L. McEuen, *Science* **344**, 1489 (2014).
- [27] J. M. Lu, O. Zheliuk, I. Leermakers, N. F. Q. Yuan, U. Zeitler, K. T. Law, and J. T. Ye, *Science* **350**, 1353 (2015).
- [28] X. Xi, Z. Wang, W. Zhao, J.-H. Park, K. T. Law, H. Berger, L. Forro, J. Shan, and K. F. Mak, *Nat Phys* **12**, 139 (2016), letter.
- [29] Y. Saito, Y. Nakamura, M. S. Bahramy, Y. Kohama, J. Ye, Y. Kasahara, Y. Nakagawa, M. Onga, M. Tokunaga, T. Nojima, Y. Yanase, and Y. Iwasa, *Nat Phys* **12**, 144 (2016), letter.
- [30] B. T. Zhou, N. F. Q. Yuan, H.-L. Jiang, and K. T. Law, *Phys. Rev. B* **93**, 180501 (2016).
- [31] N. F. Q. Yuan, K. F. Mak, and K. T. Law, *Phys. Rev. Lett.* **113**, 097001 (2014).
- [32] J. Zhang and V. Aji, (2016), [arXiv:1604.02134v2 \[cond-mat.supr-con\]](https://arxiv.org/abs/1604.02134v2).
- [33] Note that all sums over \mathbf{k} are restricted to $|\mathbf{k}|$ less than some cutoff that restricts the momentum to a single valley.
- [34] For odd parity interactions, where $v(-\mathbf{k}) = -v(\mathbf{k})$, the intravalley pairing is not excluded by symmetry. Specifically, repeating the calculation with this assumption, the intervalley terms fully cancel, and one obtains equation (8) without the intervalley term on the third line.
- [35] For example, using the values for WSe₂, $\sin^2 \theta_{\mathbf{k}} = 0.44$ and $\cos^2 \theta_{\mathbf{k}} = 0.56$ at the chemical potential.
- [36] Note that the full ground state also contains the two lower filled bands, but those contribute zero net Berry curvature and may be ignored in this section and the next.
- [37] Junhua Zhang, Evan Sosenko, and Vivek Aji, in preparation.
- [38] R. Roldán, E. Cappelluti, and F. Guinea, *Phys. Rev. B* **88**, 054515 (2013).
- [39] Related software and source code at <https://evansosenko.com/dichalcogenides>.
- [40] J. D. Hunter, *Computing In Science & Engineering* **9**, 90 (2007).